ISSN NO. 2320-5407

Journal homepage: http://www.journalijar.com

INTERNATIONAL JOURNAL OF ADVANCED RESEARCH

RESEARCH ARTICLE

Removal of Lead by Nanosized Mesoporous Aluminosilicate from aqueous systems

Ibrahim M. M. Kenawy[a], Mohamed M. Eldefrawy[a], Khaled Abou-El-Sherbini[b], Rania M. El -Tabey[a]

A) Chemistry Department, Faculty of Science, P.O.Box: 35516, Mansoura University, Mansoura, Egypt

B) Inorganic Chemistry Department, National Research Centre, Cairo, Egypt

Manuscript Info

Manuscript History:

Received: 26 September 2014
Final Accepted: 15 October 2014
Published Online: November 2014

Key words:

Corresponding Author

Ibrahim M. M. Kenawy

Abstract

This paper shows how nanoporous MCM-41 was altered by incorporation of Al ions as a speedy, simple and cheap method for modification. The mesoporous aluminosilicates were synthesized with various mole ratios of Si/Al and cetyltrimethylammonium bromide (CTAB). They were characterized by infrared, small angle XRD and scanning electron microscopy. A series of experiments were proceeded to different conditions. The adsorption capacity is extremely high in the pH range 3-6 and decreasing with decreasing pH value. Time of equilibration was monitored for 15 min. Adsorption capacity was enhanced with the increase of aluminum in the framework of the adsorbent. Adsorption behavior of lead ion on MCM-41 and mesoporous aluminosilicate was studied. Langmuir isotherm fits the experimental data very well. A thermodynamic study showed spontaneity of the sorption. Positive values of enthalpy and entropy indicate endothermic and increase in order of randomness at the solid-solution interface throughout sorption. The adsorption of lead ions onto the studied adsorbents follows pseudo-second-order kinetics.

Introduction

Pollution of the natural environment by heavy metals is a worldwide problem as these metals are non-biodegradable and bio-accumulative, and lots of them have toxic properties. Several industrial facilities such as metal plating, petroleum refining, tanneries, batteries, mining operations, electronic and chemical plants, pigments, alloys and fertilizer[1, 2] release heavy metals through their waste effluents[3]. As a result of the toxic effects and the affinity for bio-accumulation in the food chain, it is required to reduce the concentration levels of heavy metals in waters.

The conventional methods precipitation, ion exchange and adsorption have been commonly accomplished for the removal of heavy metals from water[4-8].

Lead (Pb) is also one of the potentially toxic trace metal whose physicochemical cycle has been considerably affected by human activities[4]. The manufacture of storage batteries, pigments, leaded glass, mining, metal electroplating, painting, coating, smelting, petrochemical, plumbing fuels, photographic materials, matches and explosives is the main source of lead. Regardless to this, lead is also used in insecticides, plastic water pipes, food, drinks, ointments and medicinal concoctions for flavoring and sweetening. High levels of Pb(II) are dangerous if inhaled or swallowed, and can cause long-term health risks to humans and ecosystems[9]. It mainly accumulates in muscles, bones, kidneys, and brain tissues and may cause anemia, nervous system disorders, and kidney diseases[10].The greatest risk is to fetuses, babies and young children since it hinders their normal mental and physical progress. In accordance with the lead copper rule, the U.S. EPA drinking water 90^{th} percentile action level is 15µg/dm^3. On average, it is evaluated that lead in drinking water contributes to between 10 and 20% of total

exposure (from all sources). For the purpose of environmental protection and public health, it is essential to decrease the concentration of lead in contaminated water to the permissible limits before its discharge [11-13].

Mesoporous materials with ordered pore structure, large surface area have presented promise for applications ranging from air to water purification [14, 15]. MCM-41 is a mesoporous silicate presenting hexagonally packed arrays of one-dimensional, cylindrical pores, with a uniform pore distribution, large specific surface area and large pore volume[16]. The characteristic of those mesoporous silicates suggests their potential use in the fields of adsorption, catalysis and nanotechnology owing to the large specific surface area and regular porosity[17, 18]. The modification of the mesoporous materials by several functional groups received much attention in adsorption and separation science[19-21]. The modification of MCM-41 by organic modifier is an expensive method, but modification by inorganic metal ions is simple, speedy and cheap method.

In this paper, the adsorption studies of lead on MCM-41 and modified mesoporous aluminosilicate (with Si/Al mole ratio of 10 and 20) were reported. The pH effect, time effect, and adsorption isotherm have also been studied in detail[16].

2. Experimental

2.1. Reagents

All the chemicals used were of analytical grade from E. Merck (Germany), except cetyltrimethylammonium bromide (CTAB) which was supplied by Aldrich (U.K.).

2.2. Apparatus

Organic functional groups present on the adsorbents surface before and after calcination were qualitatively measured using infrared spectroscopy. Sample discs were prepared by mixing 1 mg of the samples with 500 mg of KBr (Merck) in an agate mortar and scanned in a range from 4,000 to 400 cm^{-1} using a Jasco instrument (Model 6100, Japan) . Small-angle XRD spectra were recorded on a Bruker AXS D8 ADVANCE from 2θ 4 to 10° using CuKα source (λ = 1.54 Å). Nitrogen adsorption studies were made with a (QUANTACHROME - NOVA 2000 Series) instrument. Nitrogen adsorption and desorption isotherm of the adsorbent was determined at -196 ℃ and specific surface area was determined by applying the BET equation to the isotherm. The pore size distribution was calculated using the adsorption branch of the isotherm and the Barrett-Joyner- Halenda (BJH) formula. pH measurements were made with a pH meter (Hi 931401, HANNA and Portugal). Quantitative determination of inorganic ions was made using an inductively coupled plasma-optical emission spectrometer (ICP-OES) of Perkin Elmer/Optima 7000D was employed for the determination of target elements by atomic emission spectrometry. The scanning electron microscope (SEM) images were performed using SEM model Quanta 250 FEG (Field Emission Gun) with accelerating voltage 30 K.V., magnification 14x up to 1000000. A Perkin-Elmer model 2380 atomic absorption spectrophotometer (USA) was used with Pye Unicam (England) hollow-cathode lamps for lead.

2.3. Preaparation of MCM-41 and mesoporous aluminosilicates

For preparation of mesoporous aluminosilicate, 12 g CTAB was dissolved in 460 ml of demineralized water, the mixture was stirred for 15 min. after that 80.377 g of sodium silicate nonahydrate was added to the mixture and it was stirred for 30 min. Then for preparing two materials with different ratios of Si/Al, 1000 ml solutions of $AlCl_3$ with concentrations of 0.028 M and 0.014 M were added dropwise to obtain particular materials with mole ratios 10 and 20 respectively. The stirring was sustained for 4 h. Bulky white gelatinous precipitate was formed .The resulting gel was transferred to a plastic vessel and was left for 24 h at room temperature .Then the product was filtered, washed thoroughly with demineralized water then dried at 50°C for 6 h. For preconditioning of MCM-41 and aluminosilicate ; 9 g of each sample was was placed in a round bottled flask and 250 ml of 0.1 mol l^{-1} HNO3 was introduced and the mixtures are mechanically stirred at 80 °C for 24 h .These three mixtures were filtered ,washed with deionized water then dried at 80 °C overnight. The samples prepared was labeled as follow: AlxMCM-41 where x indicated the Si/Al molar ratio and MCM-41 indicated hexagonal ordered mesoporous silicate[22].

Composition:

30 mg (dry mass) amount of sorbent samples was dissolved in 30ml 1M. NaOH. The amounts of aluminum and silicon are determined by ICP technique.

2.4. Procedure for adsorption studies

Adsorption studies of the lead on the MCM-41, Al10MCM-41 and Al20MCM-41 adsorbents were carried out using batch method. In this procedure, 20 mg of the studied adsorbents were added to 25 mL of 10 mg L^{-1} lead ions. The pH of the solutions was adjusted with NaOH (0.1M.) and HNO_3 (0.1M.). The suspension was stirred for preselected period of time using a water shaker bath. Then it was filtered and the amount of lead ions was investigated by AAS. The percentage of lead ions that was adsorbed on the adsorbent (% uptake) was figured out by comparing its concentrations before and after adsorption C_i (mg L^{-1}) and C_f (mg L^{-1}) respectively.

$$\%\text{uptake} = \frac{Ci\_Cf}{Ci} \times 100 \quad (1)$$

The equilibrium adsorption (q_e, mmol g^{-1}) was also determined by following equation:

$$q_e = (C_i - C_f) \times \frac{V}{m} \quad (2)$$

Where V is the volume of the initial solution and m is the mass of the adsorbent.

The effect of solution pH on the adsorption behavior was investigated at room temperature. In batch experiments, 20 mg of MCM-41, Al10MCM-41 and Al20MCM-41 adsorbents were equilibrated with 25 mL solution containing 10 mg L^{-1} of lead ions at various pHs for 30 min.

In the kinetics study, 20 mg of the studied adsorbents was added to 25 mL glass flasks containing 10 ppm lead ions solutions. The suspensions were shaken at 150 rpm at room temperature and samples were taken from the solution by fast filtration at different time intervals (2-90 min.).

The effect of adsorbent dose on lead ions removal was studied by shaking 25 ml of (10 ppm) lead ions solutions containing different doses of adsorbents (0.01 g–0.1 g) for a period of 15 min. at room temperature.

The isotherm study was performed using various concentrations of metals solutions (5 - 100 ppm). A mixture of 20 mg of the adsorbent materials with 25 mL adsorbate solutions of various initial concentrations was shaken at 150 rpm for 15 min. at room temperature.

The influence of the temperature on uptake of lead ions by adsorbent material was studied by equilibrating 20 mg of samples with 25 ml aqueous solution containing different concentration of lead (II) (5-100 ppm) for 15 min. at different temperatures ranging from 293 K to 333 K.

.Desorption study were applied by different ligands such as distilled water, KCN and nitric acid for lead ions desorption.

$$\text{Desorption \%} = \frac{\textit{Amount released to solution (ppm)}}{\textit{Total adsorbed (ppm)}} \times 100 \quad (3)$$

The effect of foreign ions on the uptake % of Pb^{+2} by the studied adsorbents was examined by equilibrating 20 mg adsorbent with 20 ml of 10 ppm for Pb^{+2} ions solution containing 100 ppm of various cations and anions.

The applicability for uptake of lead ions as example of pollutants from different samples of water was investigated for concentration of 10 ppm. The sportive experiments were carried out using 25 ml of clear, filtered, uncontaminated sample solutions after adjusting their pH values to 7.0 and then add 20 mg of sorbent then shaking the mixture for 15 min. The uptake percentage of lead ions from aqueous solution is computed as presented in (1).

3. Results and discussion

3.1. Characterization of adsorbent

ICP analysis presents the composition of the 3 adsorbents which is (2.1% Al, 21.9% Si) in Al10MCM-41 and (0.94% Al, 21.2% Si) in Al20MCM-41 samples, while MCM-41 has 27.3% Si in its composition. The results are given in (Table 1).

Table 1. Synthesis and surface area data of the adsorbents.

Sample	Si/Al ratio		BET surface area(m2/g)	Pore volume(cc/g)	Average pore diameter (Å)
	Added	Found			
Al10MCM-41	10	10.43	875.945	0.415	20.287
Al20MCM-41	20	22.55	953.927	0.467	20.215
MCM-41	-	-	1047.039	0.499	20.174

The small-angle XRD patterns of the as-synthesized and calcined MCM-41, Al10MCM-41 and Al20MCM-41 are presented in Fig. 1. The small angle XRD patterns of samples display a strong diffraction at 2θ smaller than 3° which approves the formation of mesoporous MCM-41. This result is specialized for hexagonal pore structure. The slight increase in d-spacing and unit cell parameters of Al-MCM-41 compared to its pure silica analog (Table 2) submits the existence of aluminum in the framework. The increase in unit cell parameter on Al incorporation is probably owing to the replacement of shorter Si–O bonds by longer Al–O bonds in the structure. It is important to notice the shift of the reflection maximum in the patterns of the as-synthesized and calcined samples. For example, the as-synthesized Al10MCM-41 has a spacing of 38.65 Å, which over calcinations decreased to 36.18 Å. This decreasing in the d spacing value is owing to contraction of the pore structure, which occurs through the process of calcinations[23].

Table 1 also presents the specific surface area, pore volume and pore size of the samples. The existence of aluminum atoms in MCM-41 type network led to a decrease of specific surface area and total pore volume values[24].

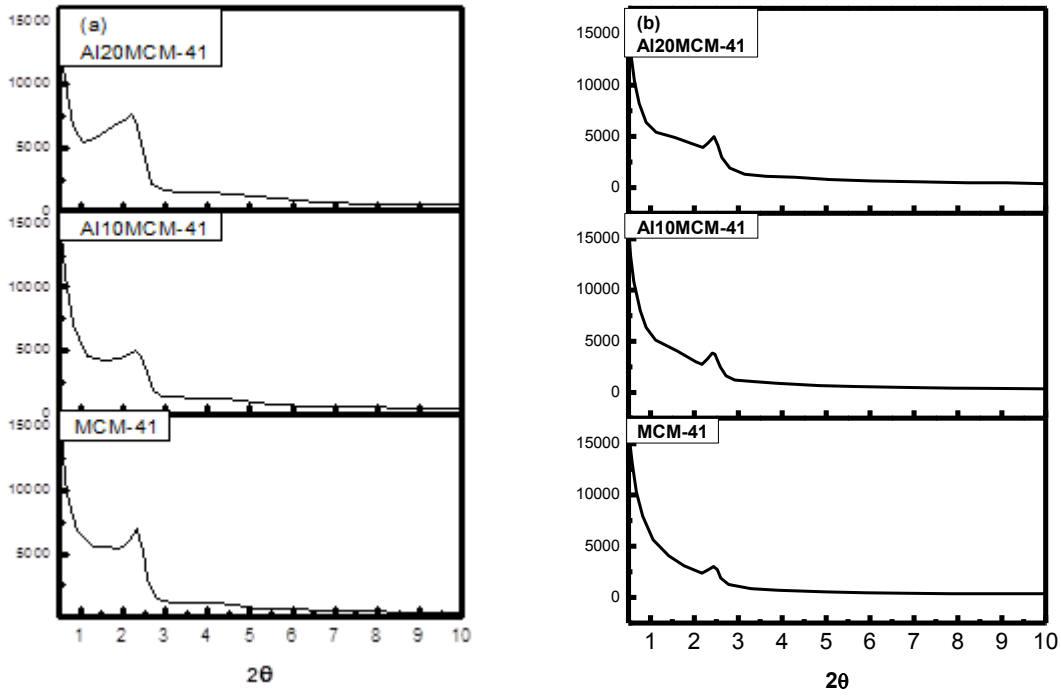

Fig. 1.Small angle XRD patterns of (a) as-synthesized and (b) calcined adsorbents.

Table 2. Physical characteristics of the adsorbents.

Sample	XRD d_{100} (Å)	Unit cell parameter [a] (a_o) (Å)	Position of 2θ
Uncalcined Al10MCM-41	38.64747	44.63	2.286
Calcined Al10MCM-41	36.18491	41.78	2.4416
Uncalcined Al20MCM-41	40.05598	46.253	2.2056
Calcined Al20MCM-41	36.30816	41.925	2.4333
Uncalcined MCM-41	38.35288	44.286	2.3036
Calcined MCM-41	36.12238	41.7105	2.4458

a. Calculated from the equation $a_{\circ} = 2d_{100}/\sqrt{3}$.

IR study of the synthesized adsorbents allowed us to identify characteristic bands of the mesoporous framework of MCM-41 and Al-MCM-41before and after removing of the template. The infrared spectra of the as-synthesized and calcined samples in the region of 400-4000 cm^{-1} is displayed in Fig. 2. As can be seen, the as-synthesized sample exhibits absorption bands around (2922, 2852, 1481 cm^{-1}) in both MCM-41 and Al10MCM-41 and bands around (2924, 2853, 1479 cm^{-1}) in Al20MCM-41 which corresponds to asymmetric and symmetric C–H stretching and C–H bending vibrations of the surfactant molecules. These bands disappear for the calcined sample indicating the total removal of organic material during calcination. Furthermore, absorption bands at 1630, 1640 and 1646 cm^{-1} in as-synthesized MCM-41, Al10MCM-41 and Al20MCM-41 respectively and also absorption bands at 1631, 1640 and 1638 cm^{-1} in calcined MCM-41, Al10MCM-41 and Al20MCM-41 respectively, are caused by deformational vibrations of adsorbed water molecules. The absorption bands at 1072, 1054 and 1057 cm^{-1} in as-synthesized MCM-41, Al10MCM-41 and Al20MCM-41 respectively are due to internal and external asymmetric Si–O stretching modes. They are shifted to higher frequencies 1090, 1076 and 1080 cm^{-1} respectively in calcined MCM-41, Al10MCM-41 and Al20MCM-41 respectively. The bands at (794, 458 cm^{-1}), (786, 444 cm^{-1}) and (788, 449 cm^{-1}) are assigned to symmetric Si–O stretching and tetrahedral Si–O bending modes in MCM-41, Al10MCM-41 and Al20MCM-41 respectively and also are slightly shifted to higher frequencies under calcination. Such positive shifts in frequencies would reflect the formation of new Si–O–Si and Si–O–Al bridges during calcination due to an increased network cross-linking and would be accounting for the lattice contraction and structural stabilization that Al-MCM-41 undergoes during calcination. Many authors have taken FT-IR bands appearing around 960 cm^{-1} in silica-based matrices containing transition metal species as evidence for the isomorphous substitution of Si atoms by heteroatoms because the band was absent in pure silicates[25]. Appearance of a large band near 3420-3454 cm^{-1} is owing to O-H stretching of surface hydroxyl groups, bridged hydroxyl groups and adsorbed water molecules[26].

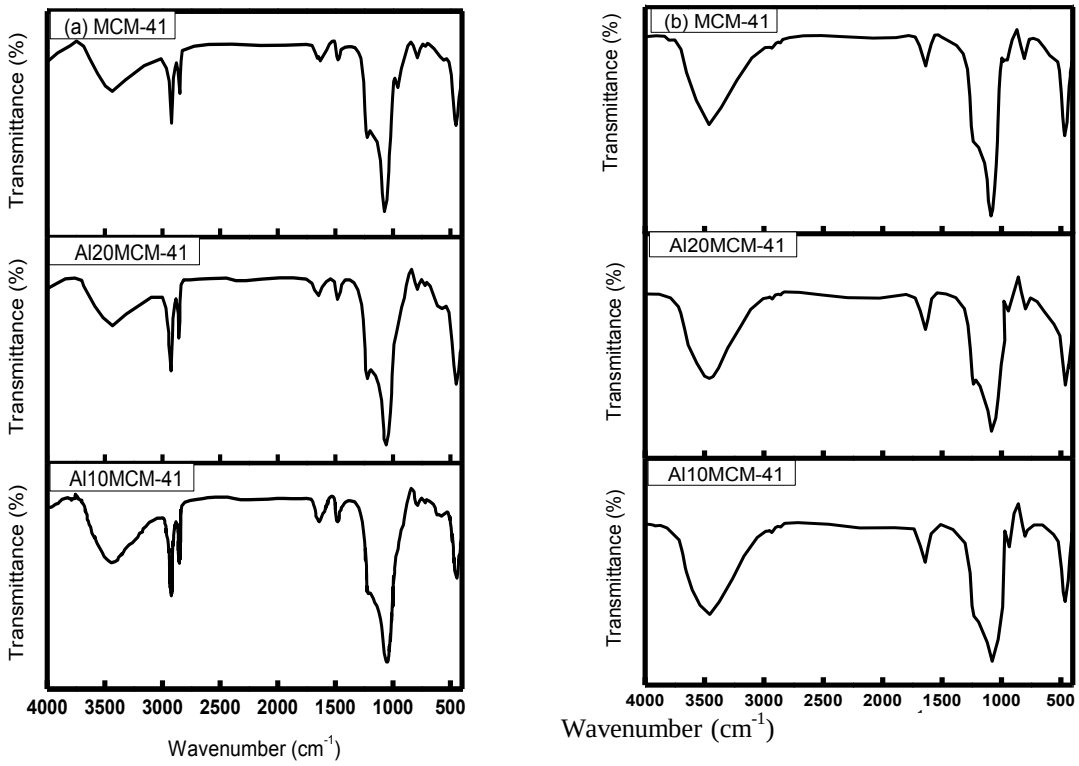

Fig. 2. IR spectrum of (a) as-synthesized and of (b) calcined adsorbents.

The morphology of the samples was studied by scanning electron microscopy (SEM) Fig. 3. SEM images present the agglomerated nanoparticles with the size range less than 100 nm[27, 28].

(a)

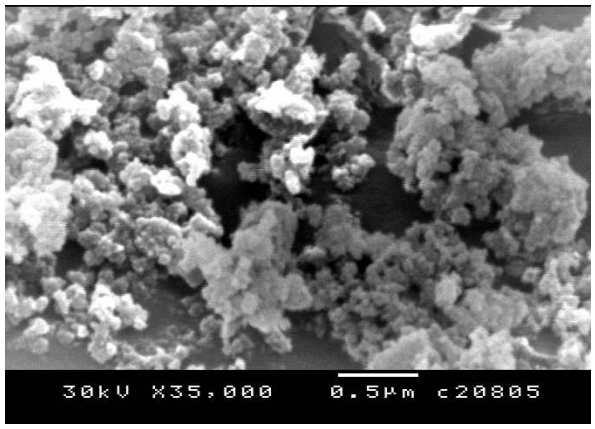

(b) **(c)**

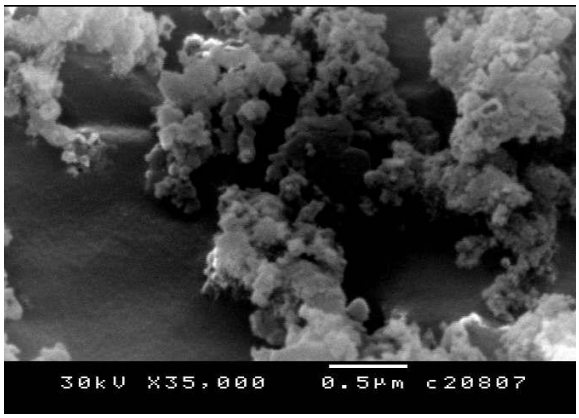

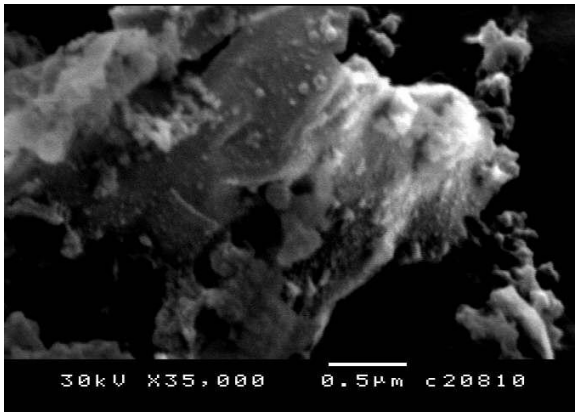

Fig. 3. SEM image of (a) MCM-41, (b) Al10MCM-41 and (c) Al20MCM-41.

3.2. Adsorption studies

Effect of pH: The adsorption of lead was studied in the pH range of 2-6. As seen in Fig. 4, the adsorption appears to be pH dependent. The uptake percent of lead ions is very high in the pH range 3-6. This may be owing to the fact that, after incorporation of aluminum, mesoporous aluminosilicate can act as an inorganic cation exchanger. It also may be owing to the fact that, in this acidic region, silanol groups onto pores were as $SiOH_2^+$ in pH<3.0. So, it was found that Pb^{+2} showed little adsorption toward MCM-41, Al10MCM-41 and Al20MCM41 in pH<3.0. At pH≥3.0 with an increase in basicity of the aqueous solution, $Si\text{-}OH_2^+$ as a cation gradually converted to a natural Si-OH by reacting with OH^-, while Pb^{+2} is only species predominant up to pH 6. Thus, adsorption of lead towards the three adsorbents was enhanced with increase in pH. The next experiments in this study were proceeded at pH=5[4].

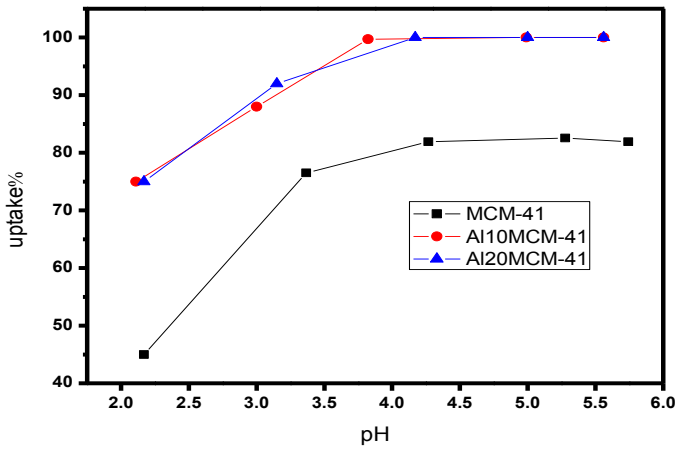

Fig. 4. Effect of pH on adsorption of Pb^{+2} onto MCM-41, Al10MCM41 and Al20MCM-41.

Kinetic study: The adsorption experiments were proceeded at initial lead concentration of 10 mg/L at pH=5. The adsorption kinetic results are shown in Fig. 5&6. It is observed that the adsorption equilibrium is attained fast in about 15 min. The fast adsorption rate suggests that the silanol groups are readily available and easily attainable probably because the uniform nanoporous channels of the adsorbents facilitate the lead ions transportation in the process. In order to clarify the adsorption kinetics of lead onto our studied adsorbents, Lagergren's pseudo-first-order and pseudo-second-order kinetic models were applied to the experimental data. The linearized form of the pseudo-first-order rate equation by Lagergren is given as:

$$\ln (q_e - q_t) = \ln q_e - K_1 t \qquad (4)$$

Where q_t and qe (mg/g) are the amount of metal ions adsorbed at t (min.) and equilibrium respectively, and K_1 is the rate constant of the equation (min^{-1}). The adsorption rate constant (K_1) can be investigated by plotting of ln ($q_e - q_t$) versus t. The plots of ln ($q_e - q_t$) versus t for the Lagergren-first-order model does not fit a pseudo-first-order kinetic model and the R^2 values for this model are extremely low 0.9045, 0.2653 and 0.265 for MCM-41, Al10MCM-41 and Al20MCM-41, respectively, for the lead adsorption by these adsorbents. Experimental data were applied also to the pseudo-second-order kinetic model which is given in the following form:

$$t/q = 1/(K_2 q_e^2) + (1/q_e)t \qquad (5)$$

Where K_2 (g/mg.min) is the rate constant of the second-order equation, q_e is the amount of adsorption equilibrium (mg/g) and q_t (mg/g) the amount of adsorption at time t (min). The linear plots of t/q_e versus t for pseudo-second-order model for the adsorption of Pb^{+2} onto MCM-41, Al10MCM-41 and Al20MCM-41are shown in Fig. 6. The rate constants (K_2), correlation coefficient of the plots together with the q_e value is given in Table 3. These results pointed out that the adsorption of lead ions onto the studied adsorbents follows very well the pseudo-second-order kinetics[29].

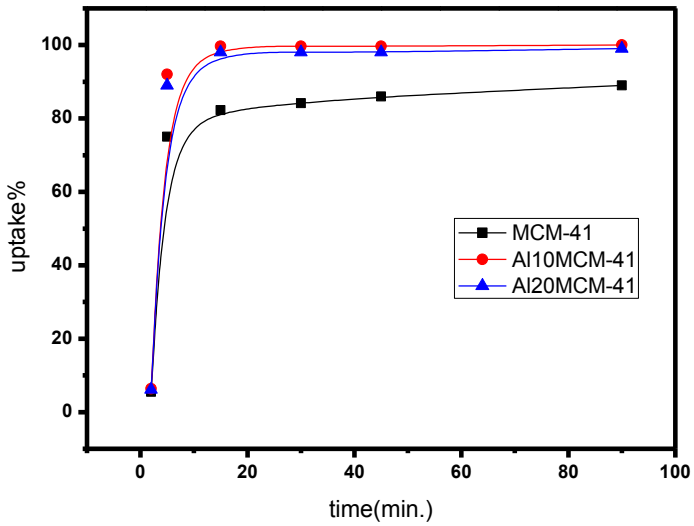

Fig. 5. Effect of contact time on adsorption of Pb^{+2} onto MCM-41, Al10MCM-41 and Al20MCM-41 at ambient temperature and C_o=10 mg/L.

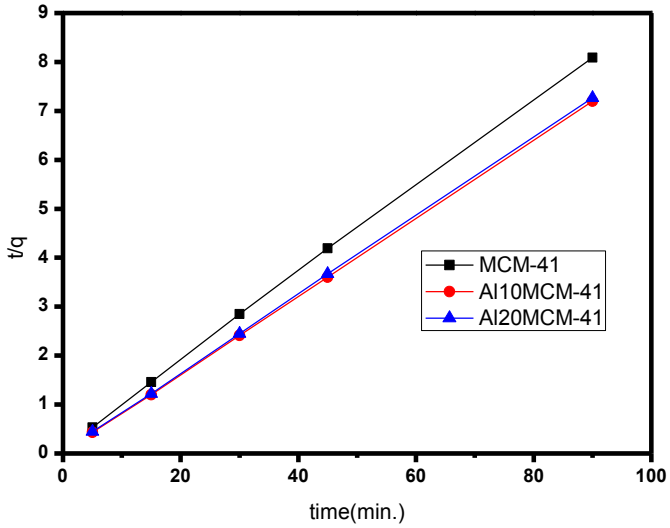

Fig. 6. Pseudo-second-order adsorption kinetic of Pb^{+2} onto MCM-41, Al10MCM41 and Al20MCM-41.

Table 3: Parameters for adsorption of Pb^{+2} onto MCM-41, Al10MCM-41 and Al20MCM-41 derived from the pseudo-first and pseudo-second-order models.

Sample	Pseudo-first-order			Pseudo-second-order		
	qe (mg/g)	$-K_1$ (min^{-1})	R^2	K_2 (g/mg.min)	qe (mg/g)	R^2
Al10MCM-41	0.43	0.07	0.27	0.383	12.54	0.99998
Al20MCM-41	0.67	0.05	0.27	0.178	12.43	0.99996
MCM-41	1.77	0.04	0.90	0.056	11.27	0.99962

Effect of adsorbent dosage: The results of the experiments with varying adsorbent concentrations are presented in Fig. 7. Increase in the adsorbent concentration from 0.01 g to 0.15 g/25 ml increases uptake % of lead (II) ions. This is due to the fact that as the adsorbent dosage is increased, more adsorption sites are available for adsorbate which cause enhancing in the percent of lead (II) uptake[30].

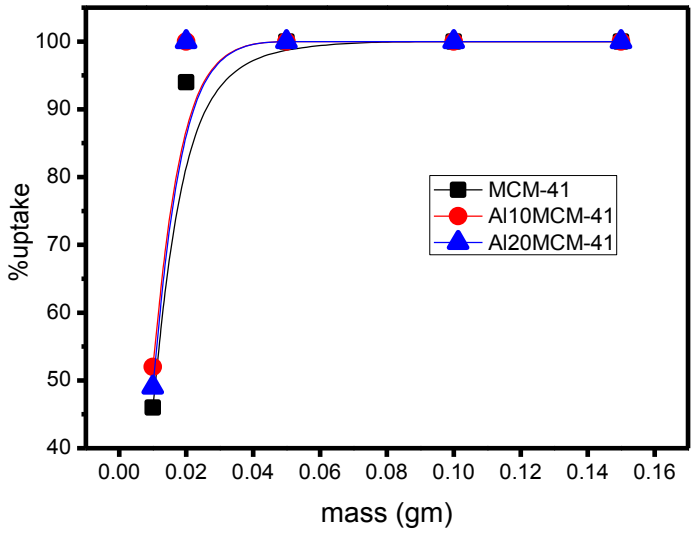

Fig. 7. Effect of MCM-41, Al10MCM-41 and Al20MCM-41 concentration on the adsorption of Pb^{+2} ions.

Effect of initial concentrations: The equilibrium isotherm shown in Fig. 8 indicated that the adsorption by all the studied adsorbents increased with the initial or equilibrium Pb ions concentrations, due to the increase in the driving force of the concentration gradient as a result of increasing the metal ion initial concentration.

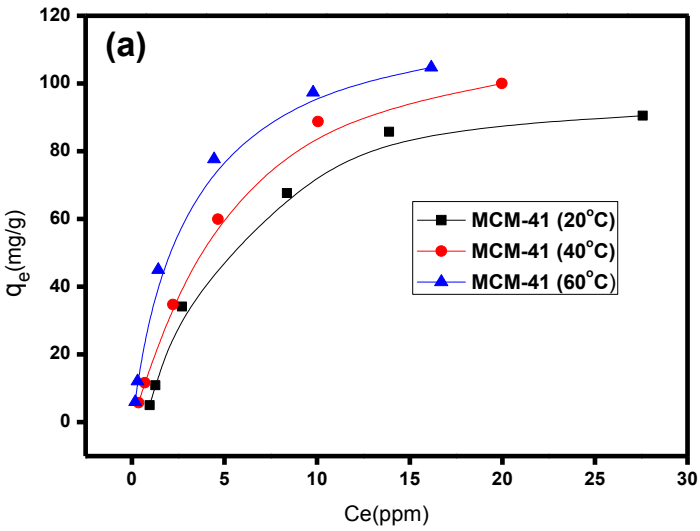

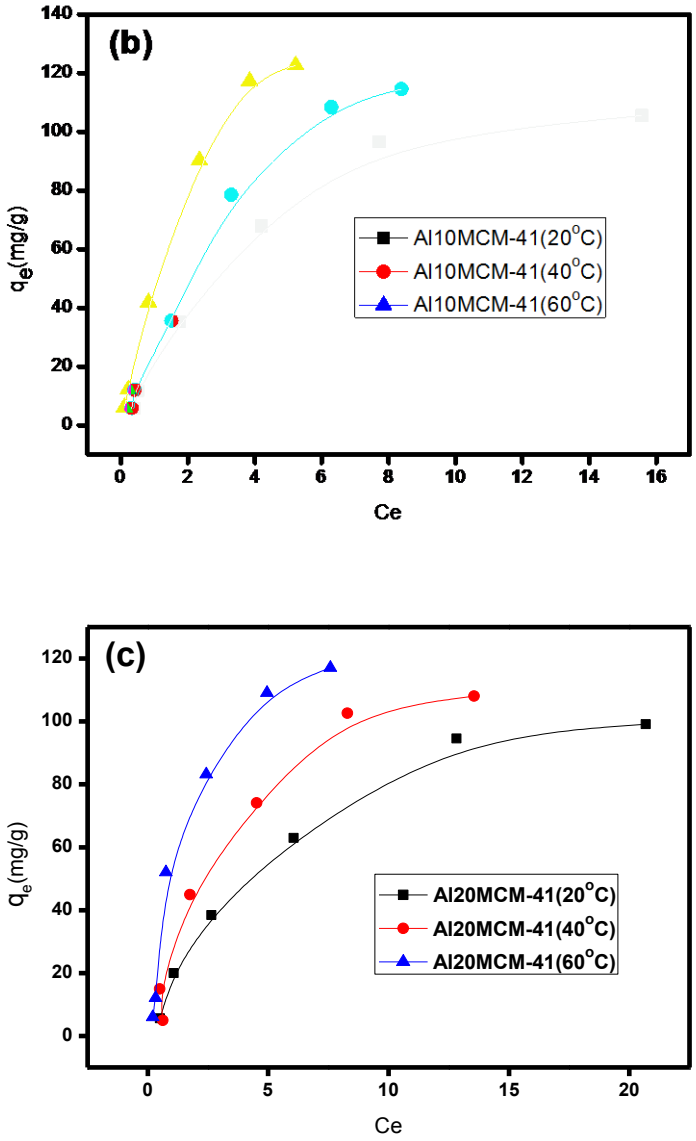

Fig. 8. Effect of initial concentration on adsorption of Pb+2 on (a) MCM-41, (b) Al10MCM-41 and (c) Al20MCM-41 at different temperatures.

Adsorption isotherm: The adsorption isotherm is plotted in Fig. 9,10. Among various binding models, Langmuir and Frendulich isotherms were employed to describe experimental data of adsorption isotherms. The Langmuir adsorption isotherm is mathematically expressed as;

$$\frac{1}{qe} = \frac{1}{bqm} + \frac{1}{Ce} \qquad (6)$$

Where b is Langmuir equilibrium constant (l/mg), and q_m (mg/g) is the monolayer adsorption capacity. Both are determined from a plot C_e/q_e versus C_e. As seen in Fig. 9, it is observed that the adsorption data fit the Langmuir equation very well and the equation constant values q_m and b, calculated from the experimental data (Table 4). Langmuir equation is the most common model employed to characterize the adsorption process in homogenous systems. For comparative purposes the experimental data have been fitted to the well-known Frendulich equation;

$$\log q_e = \log K_F + n \log C_e \quad (7)$$

Where K_F (l/g) is Freundlich constant and n is Freundlich exponent. These parameters are determined from a plot log q versus log C_e (Fig. 10). From the values of R^2 summarized in (Table 4) it is obvious that the Langmuir equation provides a better fitting than the Frendulich one[4].

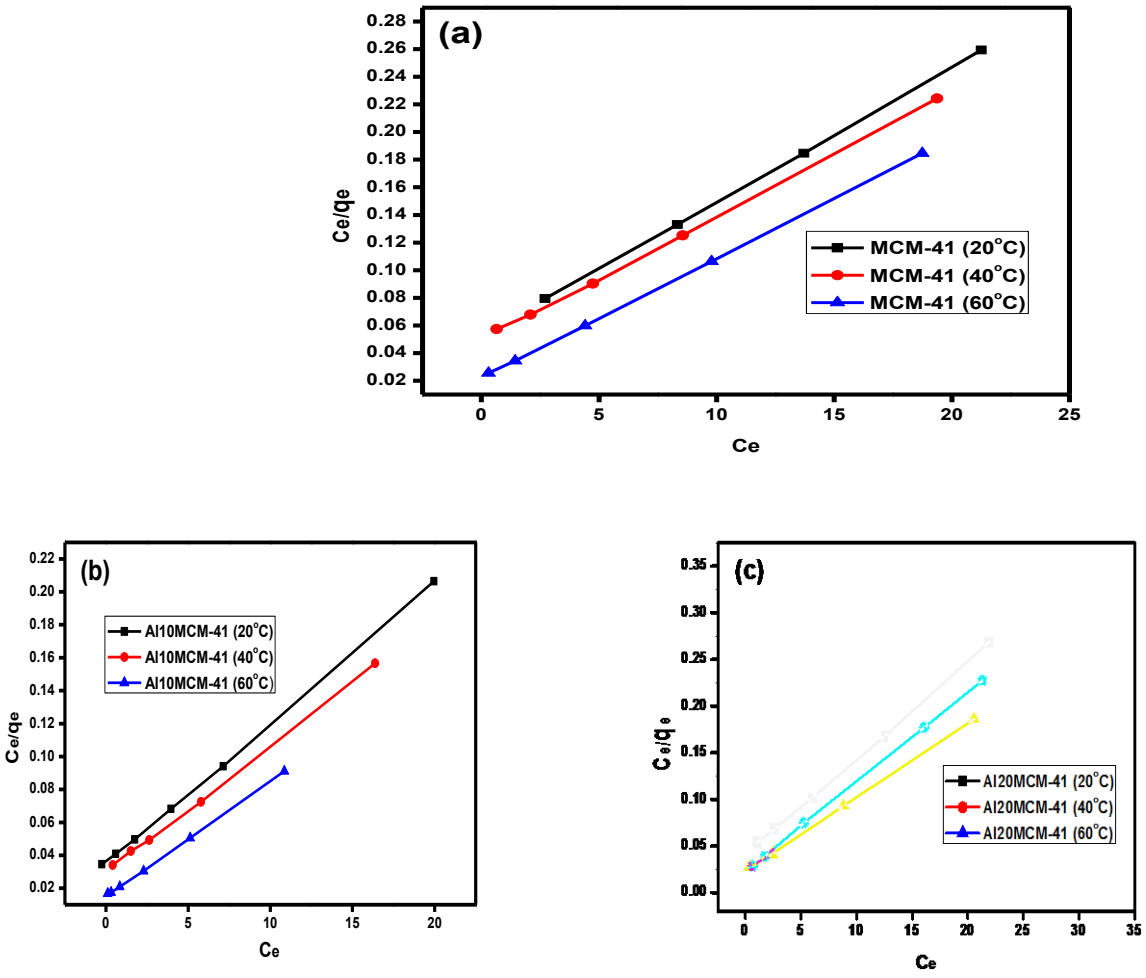

Fig. 9. Langmuir adsorption isotherm for Pb^{+2} on (a) MCM-41, (b) Al10MCM-41 and (c) Al20MCM-41.

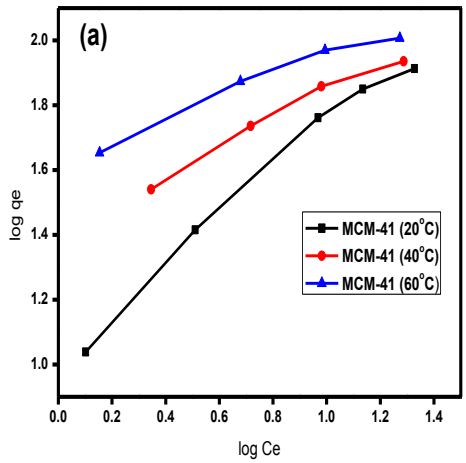

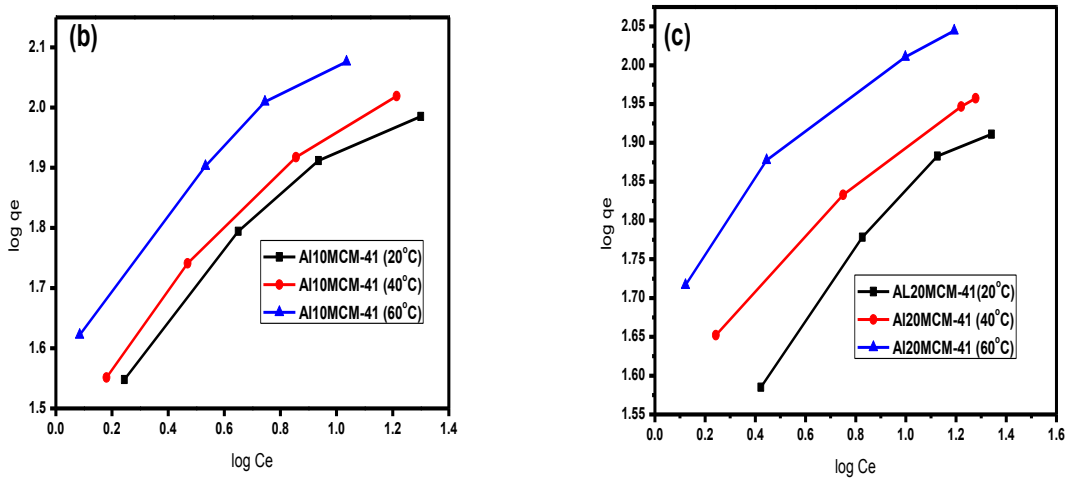

Fig. 11. Frendulich adsorption isotherm for Pb^{+2} on (a) MCM-41, (b) Al10MCM-41 and (c) Al20MCM-41.

Table 4. Fitting parameters of adsorption model isotherms.

Sample	Langmuir fitting parameters			Frendulich fitting parameters		
	R^2	b	q_m	R^2	K_f	n
Al10MCM-41						
20°C	0.9995	0.2427	117.23	0.9177	30.44	0.4167
40°C	0.9990	0.2577	129.87	0.9576	31.75	0.4495
60°C	0.9995	0.4561	143.68	0.9403	40.63	0.4901
Al20MCM-41						
20°C	0.9994	0.2507	96.899	0.9837	39.06	0.2928
40°C	0.9999	0.424	103.95	0.9433	51.06	0.2963
60°C	0.9999	0.337	126.58	0.9071	52.33	0.2688
MCM-41						
20°C	0.9998	0.1847	103.09	0.9761	10.13	0.7299
40°C	0.9993	0.1822	111.23	0.9644	25.88	0.4263
60°C	0.9999	0.3897	115.74	0.9454	42.1	0.3248

Effect of temperature: A thermodynamic study was conducted at different temperature (20°C to 60°C). The data was plotted in Van't Hoff plot as ln K_d vs. 1/T which give straight line (Fig. 11). Values of enthalpy and entropy (ΔH and ΔS) were calculated from the slope and intercept of the plot. The negative values of ΔG are signs of spontaneity of the sorption and increase in the numerical value of ΔG with increase in temperature indicates temperature favorable sorption phenomena. The positive value of enthalpy change (ΔH) confirms that the sorption process is endothermic. The positive value of entropy (ΔS) submits the increase in randomness at the solid-solution interface by the fixation of lead ions on the sorbents. Lead ions in aqueous media are hydrated. The ions were adsorbed on the adsorbents surfaces, water molecules formerly bounded to the lead ions were released and dispersed in solution, resulting in an increase in entropy. Values of thermodynamic parameters are presented in (Table 5)[30].

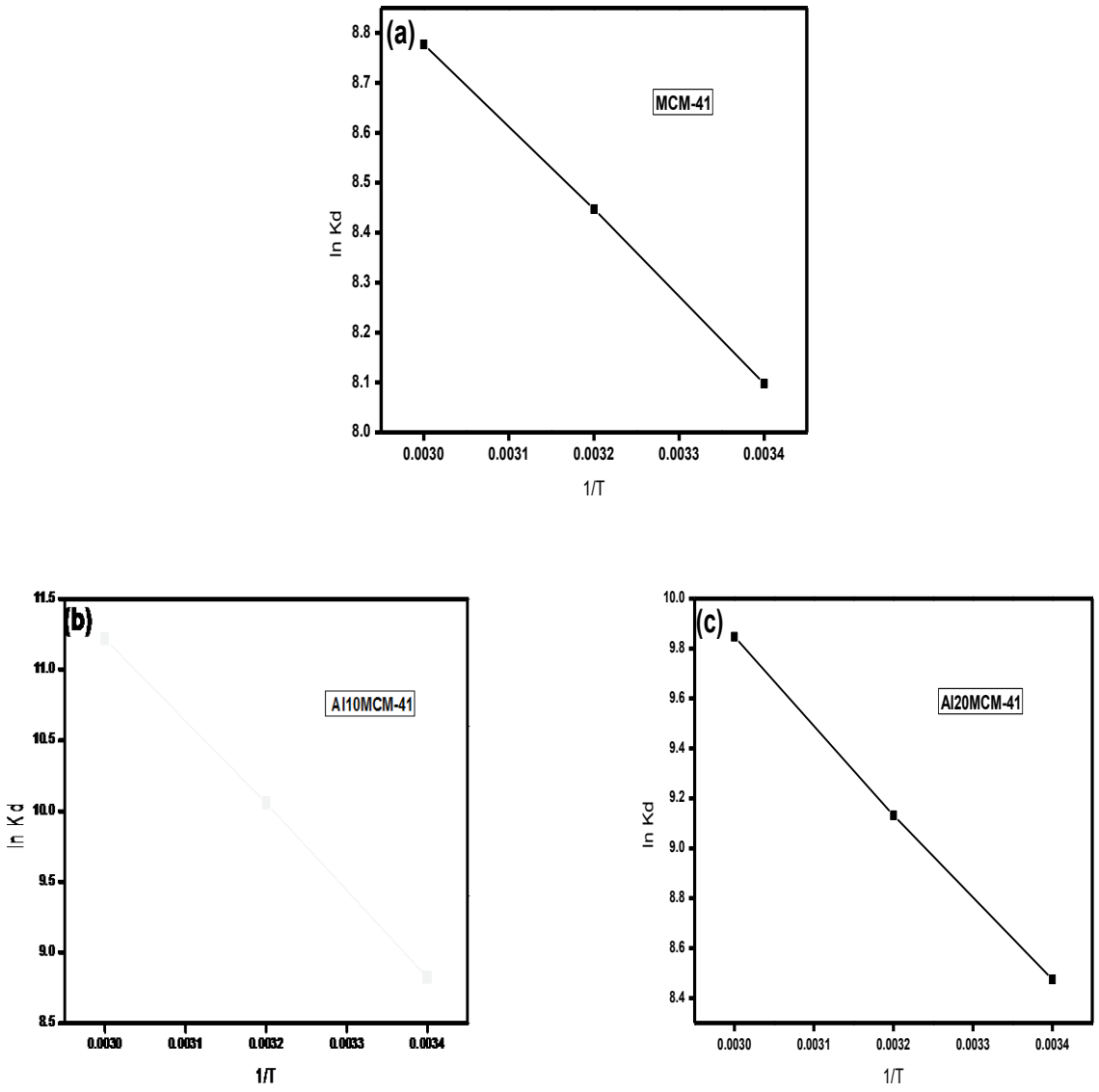

Fig. 11. Van't Hoff plot for Pb^{+2} on (a) MCM-41, (b) Al10MCM-41 and (c) Al20MCM-41.

Table 5. Thermodynamic parameters for the adsorption of Pb^{+2} on the adsorbents.

Sample	ΔG^o	ΔH^o	ΔS^o
Al10MCM-41 293 K 313 K 333 K	**-21489.92** **-24801.83** **-31050.53**	**49750.4**	**242.6**

Al20MCM-41 293 K 313 K 333 K	**-20644.78** **-23399.2** **-27260.92**	**28512.03**	**167.3**
MCM-41 293 K 313 K 333 K	**-219725.77** **-22167.02** **-24299.39**	**14118.83**	**115.4**

Desorption studies: In this study an attempt was made to investigate the desorption behavior with different ligands such as distilled water, KCN and nitric acid. Desorption study showed that distilled water and KCN has negligible desorption capacity. The results obtained from desorption study by nitric acid are given in (Table 6).

Table 6. Desorption behavior of Pb^{+2} ions on the adsorbents.

Concentration of HNO_3	**MCM-41**	**Al10MCM-41 % Desorption**	**Al20MCM-41**
0.1 M.	26.333%	31.21%	31.7%
0.3 M.	59.96%	58.81%	59.91%
1.0 M.	61.48%	62.53%	63.71%

Effect of foreign ions: Natural water matrix (anions and cations) can intensely affect the removal of heavy metals on the surface of adsorbents therefore the uptake % of Pb^{+2} by the studied samples was examined in the presence of some possible matrix ions such as phosphate , chloride, sulphate, nitrite, bicarbonate, Na^{+}, K^{+}, Mg^{+2} and Ca^{2+}. The impact of these foreign ions on the uptake% of lead ions was studied in the presence of high concentration of them to magnify their effect on the adsorption capacity of lead ions on the studied adsorbents. The results are shown in (Table 7).

Table 7. Effect of foreign ions on the adsorption of Pb^{+2}.

Foreign ion (100 ppm)	**MCM-41**	**Al10MCM-41 Uptake%**	**Al20MCM-41**
Ca^{+2}	71.8	95.34	92.22
Mg^{+2}	66.98	99.015	93.39
K^{+}	92.36	100	100
Cl^{-}	89.62	100	100
SO_4^{-2}	86.79	100	100
PO_4^{-3}	90.66	100	100
Na^{+}	76.04	97.13	94.87

NO_2^-	86.13	100	100
HCO_3^-	90.19	100	100

Analytical application: As shown in (Table 8), the applicability of the MCM-41, Al10MCM-41 and Al20MCM-41 for uptake of Pb^{+2} from different samples of natural water was studied for spiked concentration (10 ppm). The sportive experiments were carried out using 25 ml of clear, filtered, uncontaminated sample solutions after adjusting their pH values to 7.0 and then add 0.02 g of the sorbent before shaking the mixture.

Table 8. Analytical application.

Water sample	MCM-41	Al10MCM-41 % Uptake	Al20MCM-41
Ras El Bar El Gerby[e]	**74.2**	**93.3**	**87.1**
El Mansoura City[a]	**82.18**	**99.5**	**98.6**
Al Dqahlya Dekrnis[b]	**81.85**	**99.5**	**98.6**
Al Dqahlya Gamasa[e]	**77.31**	**93.5**	**93.1**
Ras El Bar Tongue[e]	**71.18**	**91.5**	**81.5**
Damietta Port Damietta[e]	**77.31**	**96**	**88**
El Manzalah Lake[c,d]	**79.83**	**98.5**	**96.3**
Al Dqahlya Meat Anter[b]	**82.44**	**98.6**	**98.4**

Note: i-All measured RSD ranges from 1-5%.
ii-a=Tap water, b=Nile water, c=Waste water, d=Lake water, e=Sea water.

4. Conclusions

MCM-41 and modified mesoporous aluminosilicate (with Si/Al mole ratios of 10 and 20) with high surface area and pore volume were synthesized. The modification of MCM-41 by aluminum ion is speedy, simple and cheap method in comparison with the modification by organic modifiers. The results showed that mesoporous aluminosilicate works as a very good adsorbent for lead ions. It is also clear that the adsorption capacity of our studied adsorbents towards lead ions is in the order of Al10MCM-41> Al20MCM-41> MCM-41.

References

1. Bailey, S.E., et al., A review of potentially low-cost sorbents for heavy metals. Water research, 1999. **33**(11): p. 2469-2479.
2. Rostamian, R., M. Najafi, and A.A. Rafati, Synthesis and characterization of thiol-functionalized silica nano hollow sphere as a novel adsorbent for removal of poisonous heavy metal ions from water: kinetics, isotherms and error analysis. Chemical Engineering Journal, 2011. **171**(3): p. 1004-1011.
3. Yuan, L. and Y. Liu, Removal of Pb (II) and Zn (II) from aqueous solution by ceramisite prepared by sintering bentonite, iron powder and activated carbon. Chemical Engineering Journal, 2013. **215**: p. 432-439.
4. Sepehrian, H., et al., Adsorption Studies of Lead on Modified Mesoporous Al-MCM-41. Ion Exchange Letters, 2011. **4**: p. 1-6.
5. Mustafa, S., et al., Solvent effect on the electrophoretic mobility and adsorption of Cu on iron oxide. Colloids and Surfaces A: Physicochemical and Engineering Aspects, 2008. **330**(1): p. 8-13.
6. Mustafa, S., et al., Chromium (III) removal by weak acid exchanger Amberlite IRC-50 (Na). Journal of hazardous materials, 2008. **160**(1): p. 1-5.
7. Tunali, S., et al., Equilibrium and kinetics of biosorption of lead (II) from aqueous solutions by< i> Cephalosporium aphidicola</i>. Separation and Purification Technology, 2006. **47**(3): p. 105-112.
8. Lao, C., et al., Sorption of Cd (II) and Pb (II) from aqueous solutions by a low-rank coal (leonardite). Separation and purification technology, 2005. **45**(2): p. 79-85.
9. Wu, X.-W., et al., Adsorption of Pb (II) from aqueous solution by a poly-elemental mesoporous adsorbent. Applied Surface Science, 2012. **258**(14): p. 5516-5521.
10. Kim, S.A., et al., Removal of Pb (II) from aqueous solution by a zeolite–nanoscale zero-valent iron composite. Chemical Engineering Journal, 2013. **217**: p. 54-60.
11. Ranđelović, M., et al., Synthesis of composite by application of mixed Fe, Mg (hydr) oxides coatings onto bentonite–a use for the removal of Pb (II) from water. Journal of hazardous materials, 2012. **199**: p. 367-374.
12. Yang, S., et al., Impact of environmental conditions on the sorption behavior of Pb (II) in Na-bentonite suspensions. Journal of hazardous materials, 2010. **183**(1): p. 632-640.
13. Ozdes, D., et al., Removal of Pb (II) ions from aqueous solution by a waste mud from copper mine industry: equilibrium, kinetic and thermodynamic study. Journal of hazardous materials, 2009. **166**(2): p. 1480-1487.
14. Idris, S.A., et al., Large pore diameter MCM-41 and its application for lead removal from aqueous media. Journal of hazardous materials, 2011. **185**(2): p. 898-904.
15. Liu, M., et al., Synthesis, characterization, and mercury adsorption properties of hybrid mesoporous aluminosilicate sieve prepared with fly ash. Applied surface science, 2013. **273**: p. 706-716.
16. Sepehrian, H., R. Cheraghali, and P. Rezaei, Adsorption behavior studies of Cerium on modified Mesoporous Aluminosilicate. International Journal of Nano Dimension, 2014. **5**(2): p. 169-175.
17. Cheng, C.-F., et al., Controlling the channel diameter of the mesoporous molecular sieve MCM-41. Journal of the Chemical Society, Faraday Transactions, 1997. **93**(2): p. 359-363.
18. Selvam, P., S.K. Bhatia, and C.G. Sonwane, Recent advances in processing and characterization of periodic mesoporous MCM-41 silicate molecular sieves. Industrial & Engineering Chemistry Research, 2001. **40**(15): p. 3237-3261.
19. Jal, P., S. Patel, and B. Mishra, Chemical modification of silica surface by immobilization of functional groups for extractive concentration of metal ions. Talanta, 2004. **62**(5): p. 1005-1028.
20. Li, J., et al., Synthesis and characterization of imidazole-functionalized SBA-15 as an adsorbent of hexavalent chromium. Materials Letters, 2007. **61**(14): p. 3197-3200.

21. Fryxell, G.E., et al., Design and synthesis of self-assembled monolayers on mesoporous supports (SAMMS): the importance of ligand posture in functional nanomaterials. Journal of Materials Chemistry, 2007. **17**(28): p. 2863-2874.
22. Sepehrian, H., et al., Adsorption studies of heavy metal ions on mesoporous aluminosilicate, novel cation exchanger. Journal of hazardous materials, 2010. **176**(1): p. 252-256.
23. Suyanta, S., et al., SYNTHESIS AND CHARACTERIZATION OF MESOPOROUS ALUMINOSILICATES Al-MCM-41 AND INVESTIGATION OF ITS THERMAL, HYDROTHERMAL AND ACIDITY STABILITY. Indonesian Journal of Chemistry, 2010. **10**(1): p. 41-45.
24. Nastase, S., et al., Ordered mesoporous silica and aluminosilicate-type matrix for amikacin delivery systems. Microporous and Mesoporous Materials, 2013. **182**: p. 32-39.
25. Eimer, G.A., et al., Synthesis and characterization of Al-MCM-41 and Al-MCM-48 mesoporous materials. Catalysis letters, 2002. **78**(1-4): p. 65-75.
26. Boukoussa, B., et al., Adsorption of yellow dye on calcined or uncalcined Al-MCM-41 mesoporous materials. Arabian Journal of Chemistry, 2013.
27. Abdollahi-Alibeik, M. and E. Heidari-Torkabad, H< sub> 3</sub> PW< sub> 12</sub> O< sub> 40</sub>/MCM-41 nanoparticles as efficient and reusable solid acid catalyst for the synthesis of quinoxalines. Comptes Rendus Chimie, 2012. **15**(6): p. 517-523.
28. Zhai, S.-R., I. Kim, and C.-S. Ha, Structural and catalytic characterization of nanosized mesoporous aluminosilicates synthesized via a novel two-step route. Catalysis Today, 2008. **131**(1): p. 55-60.
29. SEPEHRIAN, H., R. CHERAGHALI, and A.H.A. REZAEI PEYMAN, Adsorption Behavior of lanthanum on modified nanoporous aluminosilicates. INTERNATIONAL JOURNAL OF INDUSTRIAL CHEMISTRY (IJIC), 2011.
30. Bhadoria, R., B. Singh, and R. Tomar, Sorption of toxic metals on sodium aluminosilicate (NAS). Desalination, 2010. **254**(1): p. 192-200.